Peroxiredoxin 3 Inhibits Cardiac Fibrosis in Mice via NOX4-P38 Signalling

Xiaoqi Xiong, Ph.D.[1#], Jun Li, Ph.D.[1#], Zhen Chen, Ph.D.[2#], Changjun Luo, Ph.D.[1], Wei Wei, Ph.D.[1], Bing Li, Ph.D.[1],

Yi Kang, Ph.D.[1], Xiuhong Nong, Ph.D.[1], Fen Ai, Ph.D.[2*], Jing Zhang, Ph.D.[1*]

1. Department of Cardiology, Liuzhou Municipal Liutie Central Hospital, Liuzhou City, Guang Xi Province, P.R. China
2. Department of Emergency, The Central Hospital of Wuhan, Tongji Medical College, Huazhong University of Science and Technology, Wuhan City, Hubei Province, P.R. China

Abstract
Objective: Peroxiredoxin-3 (Prx-3) is widely acknowledged as an antioxidant that protects against mitochondrial reactive oxygen species. Nonetheless, its role in cardiac fibrosis has not been elucidated. We aim to explore the role and mechanism of Prx-3 in cardiac fibrosis.

Materials and Methods: In this experimental study, mice received subcutaneous injections of isoproterenol (ISO) for 14 consecutive days (10 mg/kg/d for three days, followed by 5 mg/kg/d for 11 days) to establish a cardiac fibrosis model. The mice were subsequently injected with adenovirus-Prx-3 (ad-Prx-3) to enable Prx-3 overexpression. Echocardiography was used to evaluate cardiac function. Mice heart fibroblasts were isolated and stimulated with transforming growth factor β1 (TGFβ1) to induce fibrosis in vitro. Cells were also transfected with ad-Prx-3 for overexpression of Prx-3.

Results: Echocardiographic diameters and fibrosis markers indicated that Prx-3 could inhibit ISO-induced cardiac dysfunction and fibrosis. Fibroblasts with Prx-3 overexpression exhibited reduced activation, proliferation, and collagen transcription. We found that Prx-3 reduced the expression of NADPH oxidase 4 (NOX4) and reduced P38 levels. After treatment with a P38 inhibitor, the Prx-3 overexpression-induced anti-fibrosis effect was mitigated.

Conclusion: Prx-3 could protect against ISO-induced cardiac fibrosis by inhibiting the NOX4-P38 pathway.

Keywords: Cardiac Fibrosis, Isoproterenol, NADPH Oxidase 4, Peroxiredoxin 3, P38

Introduction

Myocardial fibrosis represents the compensatory response of the heart after myocardial injury to maintain the integrity of cardiac structure and function (1). However, persistent myocardial fibrosis and massive accumulation of extracellular matrix can lead to cardiac interstitial expansion and affect normal electrical conduction and diastolic function (2). In most cardiovascular diseases, myocardial fibrosis is associated with poor prognoses (3). It is widely acknowledged that cardiomyocytes are terminally differentiated cells. Once the myocardium is damaged, the injured cardiomyocytes can only be healed through scarring (4). During injury, fibroblasts rapidly differentiate into myofibroblasts and secrete a large amount of collagen-based extracellular matrix to maintain cardiac function (5). However, the long-term activation of new myofibroblasts and the accumulation of extracellular matrix lead to increased myocardial stiffness, cardiac dysfunction, and heart failure (6).

In various cardiovascular diseases, activation of the neuroendocrine system leads to the secretion of pro-inflammatory and pro-fibrosis factors (7), which causes myocardial injury and stimulates subsequent fibrosis. Therefore, research on the prevention and treatment of myocardial fibrosis after myocardial injury plays an important role in preventing and treating heart failure induced by various causes.

Peroxiredoxin-3 (Prx-3) is a member of the peroxidase family whose main function is to remove peroxides from tissues and cells (8). Prx-3 is mainly located in mitochondria (9). As the main site of oxidative phosphorylation of energy, mitochondria are the main subcellular structure for peroxide production (10). It has been found that Prx-3 can eliminate the

Royan Institute
Cell Journal (Yakhteh)

excess peroxide in mitochondria to counter antioxidant stress (11). Prx-3 can protect various tissues and organs from oxidative stress injury, including lung tissues, liver, and intestinal ischemia (12). The results of recent studies show that Prx-3 can protect against various cardiovascular diseases. According to Sonn et al. (10), mice that lacked Prx-3 had evidence of mitochondrial dysfunction, cardiac hypertrophy, and heart failure. Arkat et al. (11) reported that Prx-3 could protect cardiomyocytes from high glucose-induced injury in a diabetic cardiomyopathy model. However, the role of Prx-3 in cardiac fibrosis remains unclear. In this study, we use an isoproterenol (ISO)-induced mice cardiac injury model to elucidate the effects of Prx-3 on cardiac fibrosis and fibroblasts.

Materials and Methods

Compliance with ethical standards

In this experimental study, the Institutional Animal Care and Use Committee of Guangxi Medical University (2021-06223, Guangxi, China) approved all our animal experiments. All animal studies were performed in compliance with the "Animal Research: Reporting of In Vivo Experiments" (ARRIVE) guidelines (NIH Publication, revised 2011).

Animal model

Male C57BL6J mice (aged 8-10 weeks, 23.5-27.5 mg) were provided and raised at the SPF Laboratory Animal Centre of Guangxi Medical University. The cardiac fibrosis mice models were established as previously described (13). Briefly, mice were subjected to subcutaneous ISO injections (10 mg/kg/d for three days, followed by 5 mg/kg/d for 11 days). Mice in the control group were injected with the same volume of normal saline (NS). One week before the ISO injections, the mice received an injection of adeno-associated virus 9 (AAV9)-Prx-3 to overexpress Prx-3. The mice were also injected with AAV9-NOX4 to overexpress NOX4 (n=12 per group). A total of 72 mice were used in this study.

Adeno-associated virus vector

Vigene Bioscience Company (Shanghai, China) provided us with AAV9-Prx-3, AAV9-NOX4, and the negative control (AAV9-NC). All of the adeno-associated virus vectors were constructed with 1395-bp periostin promoter to induce fibroblast-specific gene delivery. One week before the ISO injections, the mice were injected with AAV9-Prx-3 or AAV9-NOX4 (60-80 ml, $5.0-6.5 \times 10^{13}$ VG/ml) through the tail vein.

Echocardiographic evaluation

An ultrasonic cardiography was carried out as previously documented (14). We removed the chest hair of the mice by shaving and subsequently anesthetized them with isoflurane (1.5%). After no response to stimulation of the mouse's feet, a 10 MHz linear array ultrasonic transducer was used for ultrasonic detection, and the data for ventricular cavity size and thickness were collected by M-mode echocardiography. The left ventricular ejection fraction (LVEF) and left ventricular shortening fraction (LVFS) were calculated.

Picrosirius red staining

Picrosirius red (PSR) staining of heart tissue was used to visualize collagen deposition (15). The heart tissue was dehydrated and embedded in paraffin. Histopathological sections were dehydrated with a series of alcohol. Then, collagen in the heart tissues was stained by PSR and photographed under a microscope. The collagen area was analysed by Image-Pro Plus 6.0, and six hearts in each group were stained.

Isolation and culture of adult mice fibroblasts

Mice (aged 4-6 weeks) were sacrificed, and their hearts were quickly harvested. After anticoagulation with heparin, the hearts were placed in pre-cooled phosphate buffered saline (PBS) solution; the atrium was removed, the ventricles were cut into 1-3 mm^3 tissue blocks and digested four times (15 minutes each) with 0.125% trypsin EDTA (Gibco, USA). The tissue was collected and digested in DMEM-F12 that contained 15% foetal bovine serum (Gibco, USA). The digestive juice was collected via centrifugation and the cell mass was filtered after centrifugation. The filtered cells were resuspended in DMEM-F12 medium and subsequently inoculated on a 10-cm petri dish. After 90 minutes, non-adherent cells in the upper layer were removed, and the fibroblasts that had adhered to the bottom of the culture dish were collected. α-smooth muscle actin (α-SMA) staining was used determine the purity of the fibroblasts. The cells were transfected with adenovirus (ad-Prx-3) or Prx-3 siRNA to overexpress or knock down Prx-3 (Vigene Bioscience, Jinan, China). Then, the cells were stimulated with transforming growth factor β1 (TGFβ1, 10 ng/ml) (16) for 48 hours to induce fibroblast activation.

Western blot and real-time polymerase chain reaction

We isolated the total proteins in the cardiomyocytes or heart tissue and conducted protein electrophoresis by sodium dodecyl sulfate polyacrylamide gel electrophoresis (SDS-PAGE). The protein was transferred to immobilized membranes (Millipore, Billerica, MA, USA), which were incubated with the corresponding primary antibodies that included total (T) P38 (1:1000 dilution, #ab178867) and phosphorylated (P-) P38 (1:1000 dilution, Abcam #ab4822), NADPH oxidase 4 (NOX4, 1:1000

dilution, #ab154244) and glyceraldehyde-3-phosphate dehydrogenase (GAPDH, 1:1000 dilution, Cell Signalling Technology, #5174). After incubation with the secondary antibody, the blots were developed with enhanced chemiluminescence reagents (Bio-Rad, Hercules, CA, USA) and captured by a ChemiDoc MP Imaging System (Bio-Rad). GAPDH was used as an internal reference protein.

Total RNA from mouse heart tissue or cardiomyocytes was extracted. We reverse transcribed 2 μg of mRNA into cDNA with a cDNA Synthesis Kit (Roche Diagnostics). A Light cycler 480 instrument (software version 1.5, Roche) and SYBR Green PCR premix (Roche) were used for the amplification reaction. *GAPDH* was used as an internal reference gene to standardize and quantify gene expressions.

Immunofluorescence staining

Cells were fixed with 4% paraformaldehyde, permeabilized with 0.2% Triton X-100, then incubated with the following primary antibodies: α-SMA (Abcam, #ab7817) or proliferating cell nuclear antigen (PCNA, Abcam, #ab29). Secondary antibodies such as Alexa FluorH 568/488 goat anti-rabbit Immunoglobulin IgG (Invitrogen Life Technologies, USA) were used. The nuclei were stained with DAPI. A fluorescence microscope (Olympus DX51, Japan) was used to take photographs.

Statistical analysis

All data were expressed as mean ± SD. Comparisons between the two groups were conducted with the unpaired student's t test. Comparison among multiple groups was analysed by multivariate analysis of variance and the post-hoc Tukey test. $P<0.05$ indicated statistical significance.

Results

Effect of peroxiredoxin-3 on isoproterenol-induced cardiac fibrosis

The mice were injected with AAV9-Prx-3 to overexpress Prx-3 in the fibroblasts (Fig.1A). We observed upregulation of Prx-3 mRNA in cardiac fibroblasts (CF) isolated from the hearts injected with AAV9-Prx-3. The level of Prx-3 in cardiomyocytes isolated from these mice was comparable with the NC group (Fig.1B). There was an increase in left ventricular (LV) collagen volume in the ISO group, while Prx-3 overexpression reduced the LV collagen volume (Fig.1C). We quantified the transcription of fibrosis markers collagen I, collagen III, and connective tissue growth factor (CTGF) and observed an increase in these markers in the ISO group; there was reduced Prx-3 overexpression after the ISO injection. Echocardiography evaluation of cardiac function indicated an increased heart rate in the two ISO groups; Prx-3 overexpression did not change the heart

rate (Fig.1D). LVEF and LVFS were sharply decreased in the ISO group compared with the NS group. Prx-3 overexpression increased LVEF and LVFS in mice post-ISO injection. The ratio of mitral peak flow velocity in early diastole to peak flow velocity in late diastole (E/A) was decreased in mice that received the ISO injection and increased following Prx-3 overexpression (Fig.1E, F).

Peroxiredoxin-3 overexpression in fibroblasts inhibits transforming growth factor β1-induced fibroblast activation and function

In order to confirm the effects of Prx-3 on fibroblasts, we transfected the cells with Ad-Prx-3 to overexpress the Prx-3 protein (Fig.2A). Cell counts showed an increase in cell proliferation in the TGFβ1 group. In addition, Prx-3 inhibited cell proliferation (Fig.2B). Immunofluorescence staining showed that TGFβ1 caused an increase in α-SMA expression, whereas Prx-3 inhibited α-SMA expression (Fig.2C). RT-PCR results showed that TGFβ1 increased mRNA levels of collagen I, collagen III, and CTGF compared with the control group. In contrast, overexpression of Prx-3 inhibited their expression (Fig.2D). The cells were stained with PCNA to evaluate cell proliferation. Cells with TGFβ1 stimulation had more PCNA-positive cells, whereas cells in the Ad-Prx-3+TGFβ1 group exhibited decreased PCNA-positivity (Fig.2E).

Peroxiredoxin-3 silencing in fibroblasts mitigated transforming growth factor β induced fibroblast activation and function

It has not been determined if Prx-3 inhibition of fibroblasts can increase cell activation and function. Therefore, we transfected the cells with Prx-3 siRNA to silence the Prx-3 protein (Fig.3A). The cell counting assay results showed an increase in cell proliferation in the TGFβ1 group and Prx-3 silencing potentiated cell proliferation (Fig.3B). TGFβ1 caused an increase in α-SMA expression and Prx-3 knockdown also increased α-SMA expression (Fig.3C). RT-PCR results showed that TGFβ1 increased mRNA levels of collagen I, collagen III, and CTGF compared with the control group; Prx-3 silencing caused enhanced expression of those markers (Fig.3D). Cells with TGFβ1 stimulation had more PCNA-positive cells. There were more PCNA-positive cells observed in the Prx-3 siRNA+TGFβ1 group than in the ScRNA+TGFβ1 group (Fig.3E).

NADPH oxidase 4-P38 pathway is the target of peroxiredoxin-3 in fibroblasts

Next, we sought to explore the mechanism that underlies the inhibitory effect of Prx-3 on cardiac fibrosis by detecting the potential signalling pathways that may be involved. We observed an increase in NOX4 in the ISO group, whereas Prx-3 inhibited NOX4 expression. The pro-fibrosis molecule P38 was also activated in the ISO mice hearts and inhibited in the AAV9-Prx-3 group (Fig.4A, B).
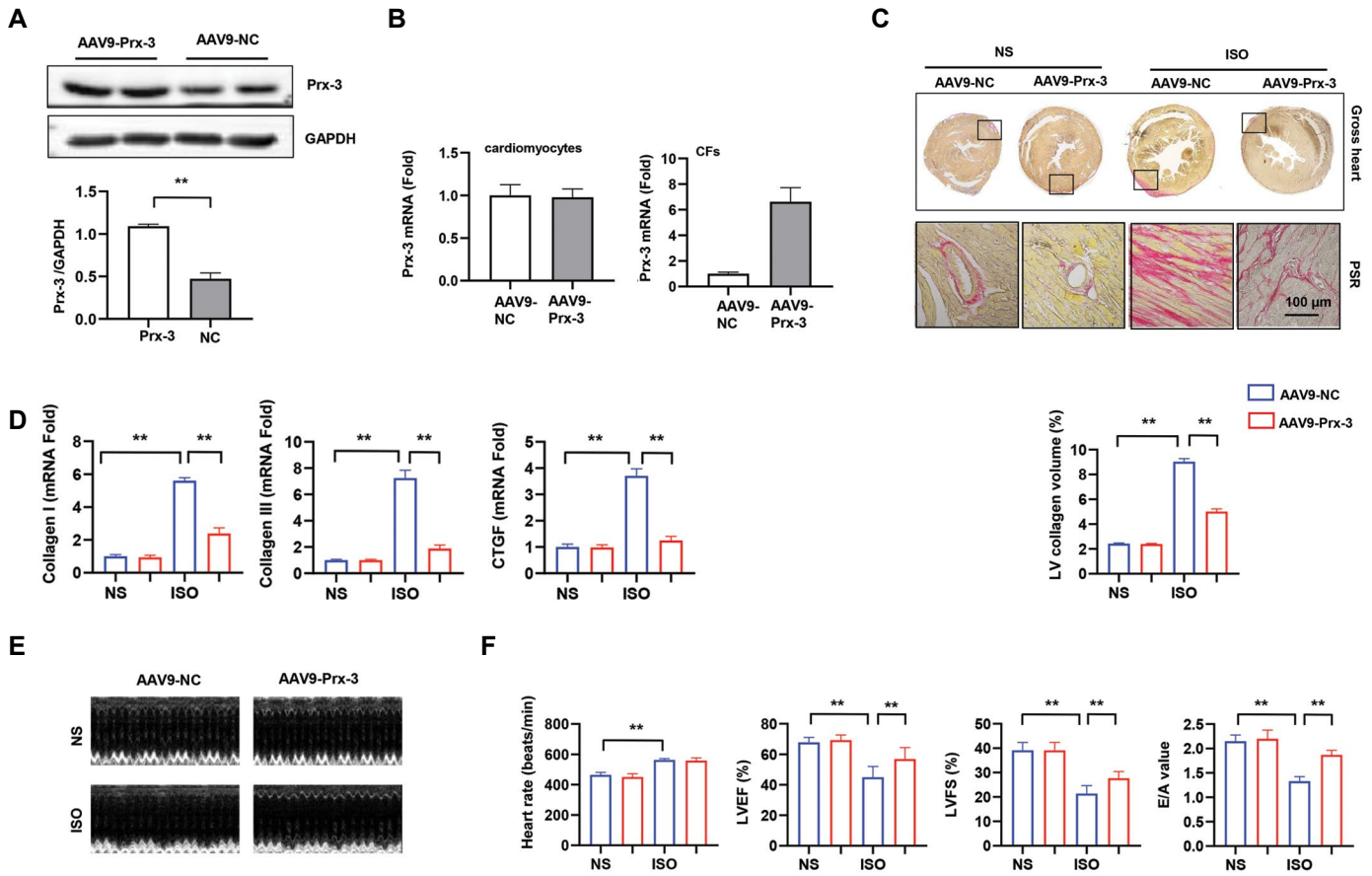
Fig.1: The effect of Prx-3 on ISO-induced cardiac fibrosis in mice. **A.** Protein level of Prx-3 in mice hearts after an AAV9-Prx-3 injection (n=4). **B.** mRNA level of Prx-3 in cardiomyocytes and CF isolated from mice hearts injected with AAV9-Prx-3 (n=6). **C.** Representative images for PSR staining and quantified results for LV collagen volume in mice hearts after ISO injection (n=6). **D.** mRNA level of fibrosis markers in mice hearts after ISO injection (n=6). Representative **E.** Echocardiographic images in each group and **F.** Measurements in mice hearts ISO injection (n=10). Prx-3; Peroxiredoxin-3, ISO; Isoproterenol, AAV9; Adeno-associated virus 9, CF; Cardiac fibroblasts, PSR; Picrosirius red, LV; left ventricular, and **; $P<0.01$ vs. control group.
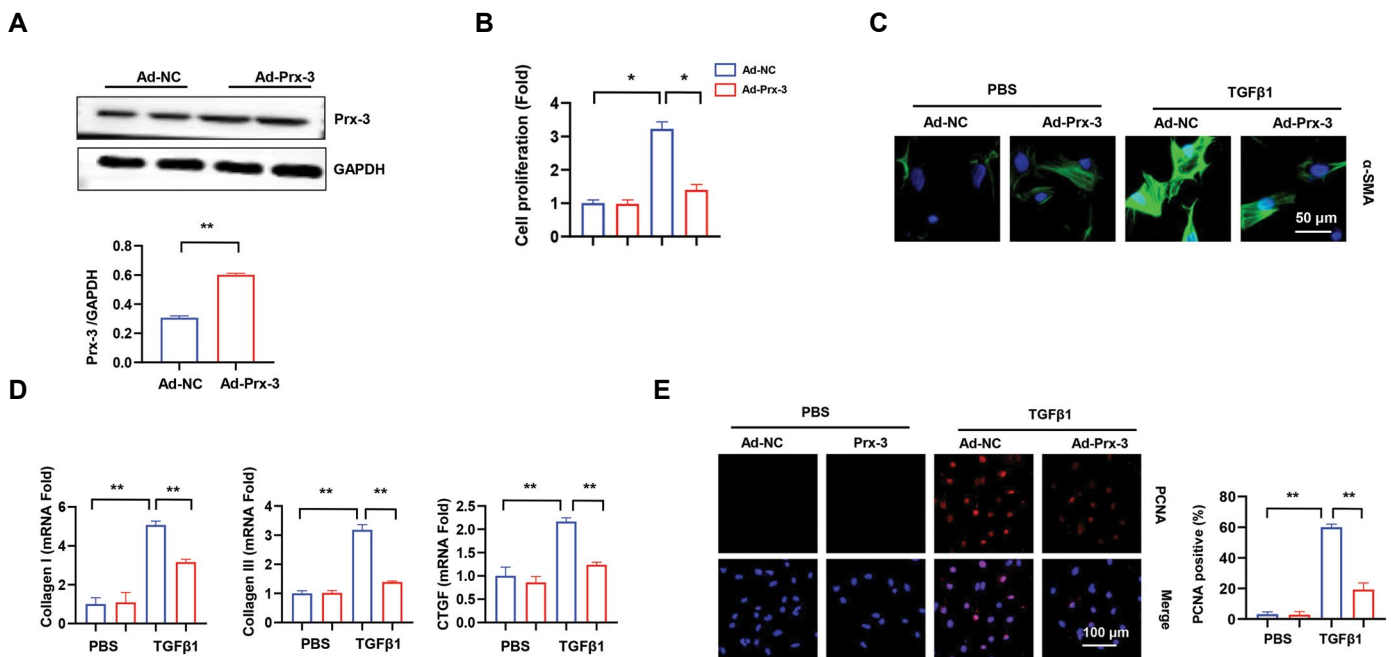

Fig.2: Prx-3 overexpression in fibroblasts inhibits TGFβ1-induced fibroblast activation and function. **A.** Protein level of Prx-3 in fibroblasts after Ad-Prx-3 transfection (n=4). **B.** Cell counts in fibroblasts after TGFβ1 stimulation (n=6). **C.** α-SMA staining results of fibroblasts after TGFβ1 stimulation (n=5). **D.** mRNA level of fibrosis markers in fibroblasts after TGFβ1 stimulation (n=6). **E.** PCNA (red) and nuclear (blue) staining results of fibroblasts in cells transfected with Ad-Prx-3 and stimulated with TGFβ1 (n=5). Prx-3; Peroxiredoxin-3, TGFβ1; transforming growth factor β1, Ad; Adenovirus, α-SMA; α-smooth muscle actin, *; $P<0.05$ vs. control group, and **; $P<0.01$ vs. control group.
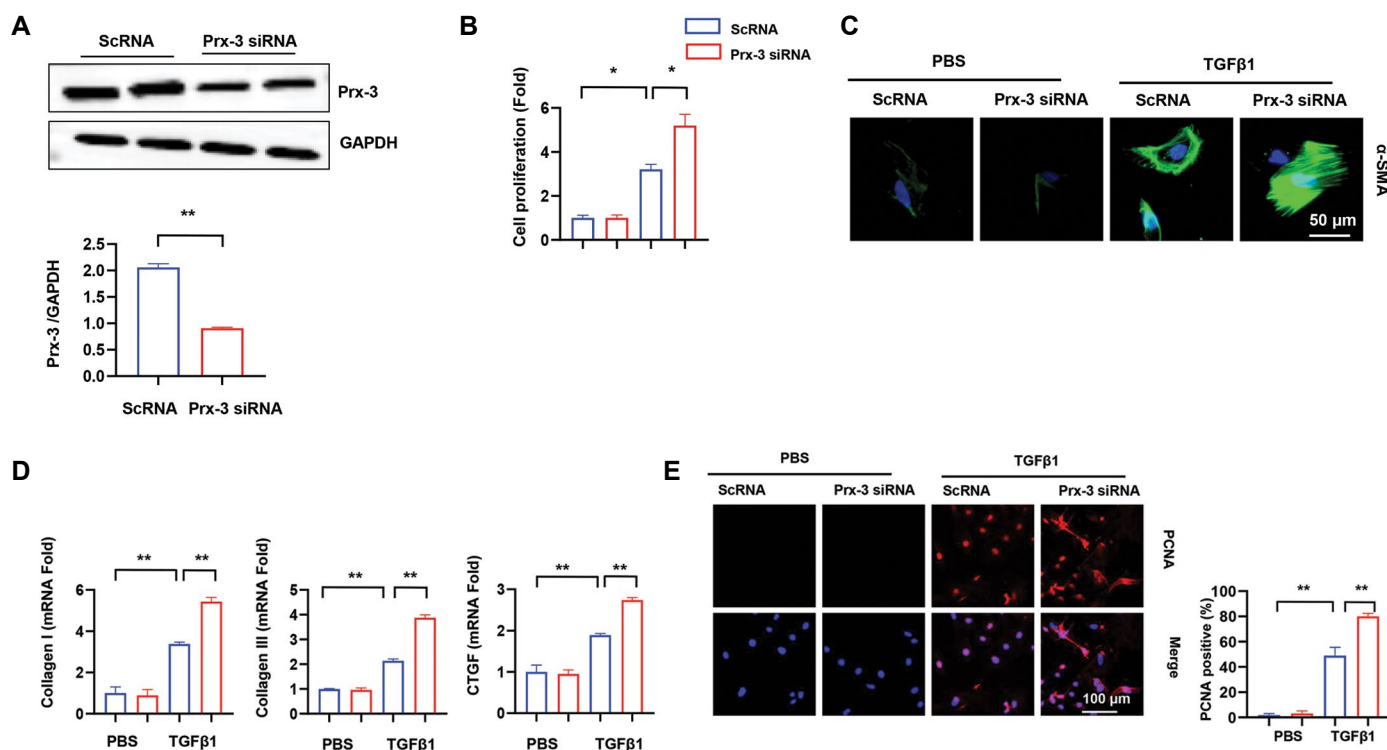
Fig.3: Prx-3 silencing in fibroblasts mitigated TGFβ1-induced fibroblast activation and function. **A.** Protein levels of Prx-3 are reduced in fibroblasts after Prx-3 siRNA transfection (n=4). **B.** Cell count assay shows an increase in proliferation in fibroblasts transfected with Prx-3 siRNA after TGFβ1 stimulation (n=6). **C.** α-SMA staining shows increased α-SMA levels in fibroblasts transfected with Prx-3 siRNA after TGFβ1 stimulation (n=5). **D.** mRNA level of fibrosis markers in fibroblasts after TGFβ1 stimulation (n=6). **E.** PCNA staining shows increased PCNA levels in fibroblasts transfected with Prx-3 siRNA after TGFβ1 stimulation (n=5). Prx-3; Peroxiredoxin-3, TGFβ1; Transforming growth factor β1, PCNA; Proliferating cell nuclear antigen, α-SMA; α-smooth muscle actin, *; P<0.05 vs control group, and **; P<0.01 vs control group.
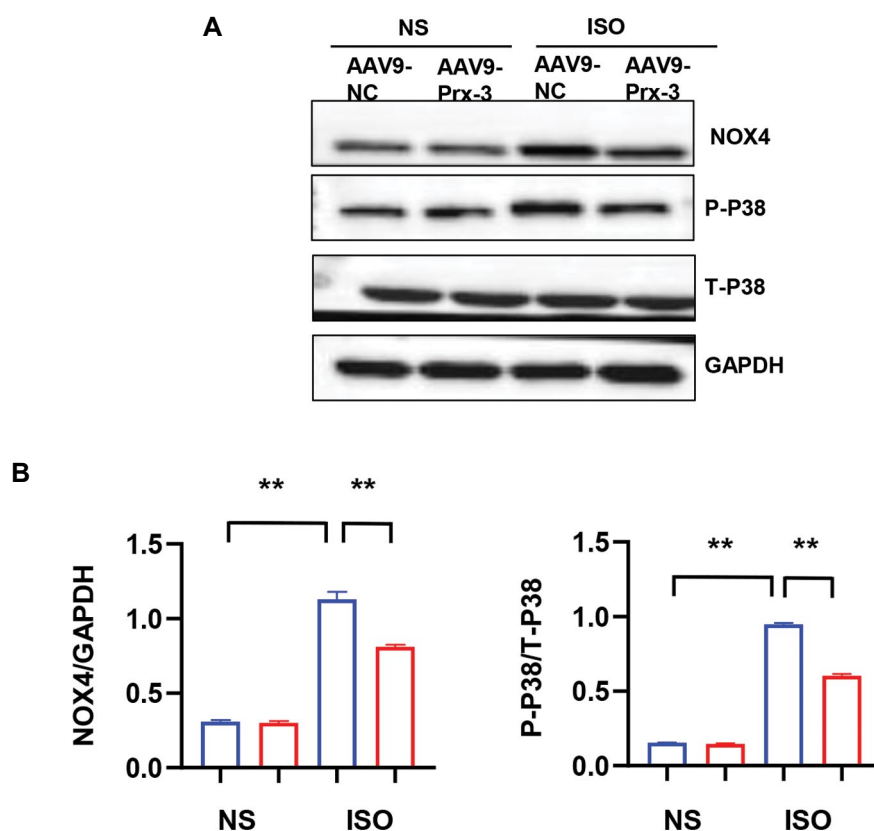

Fig.4: NOX4-P38 pathway is the target of Prx-3 in fibroblasts. **A, B.** Protein levels of NOX4, and total P38 and P-P38 in mice hearts after AAV9-Prx-3 injection (n=4). NOX4; NADPH oxidase 4, Prx-3; peroxiredoxin-3, AAV9; adeno-associated virus 9, and **; P<0.01 vs. control group.
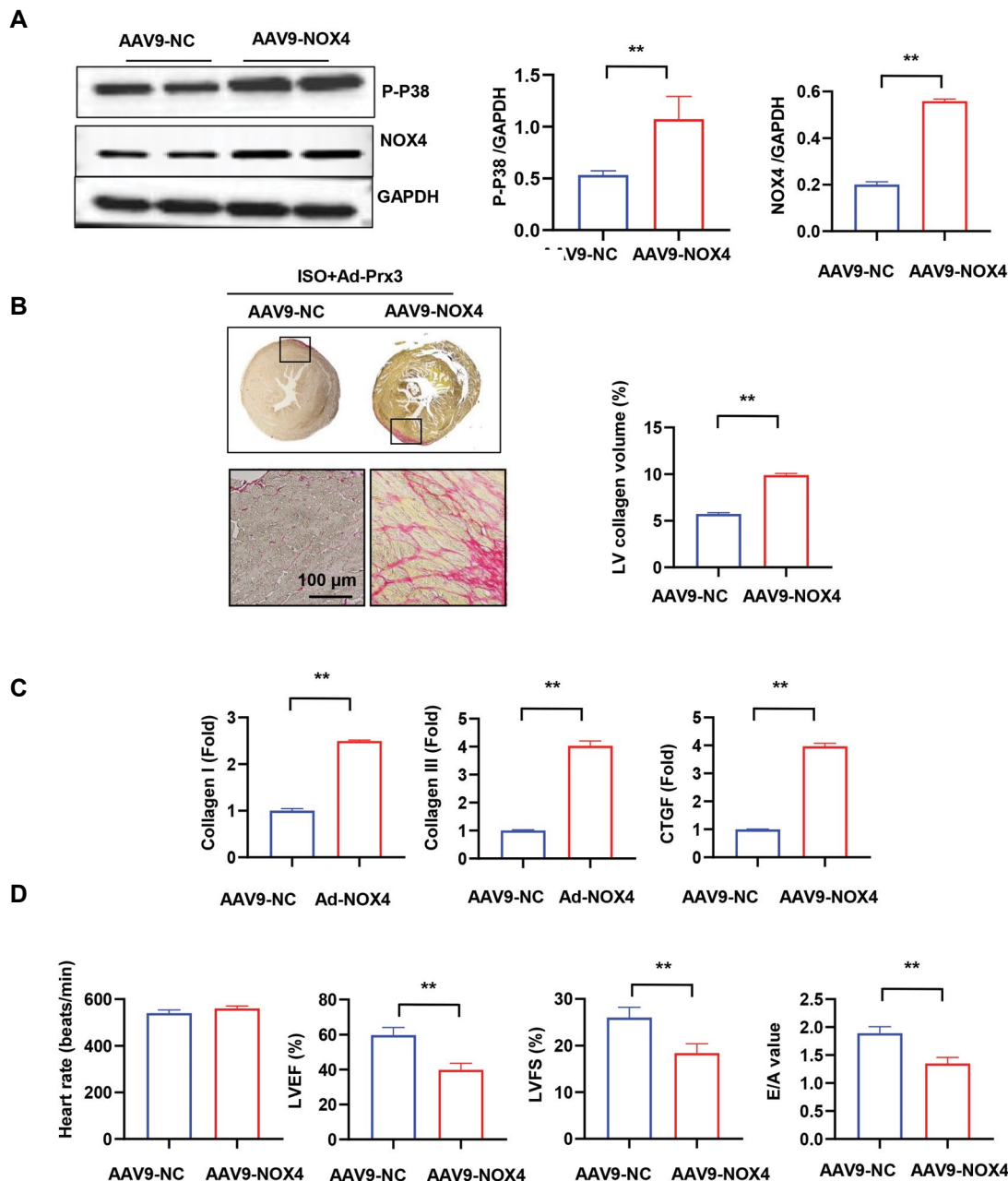
Fig.5: NOX4 overexpression mitigates the anti-fibrosis effects of Prx-3. **A.** Protein levels of NOX4 and P-P38 in mice hearts after AAV9-NOX4 injection (n=4). **B.** Representative image for PSR staining and quantified LV collagen volume results in mice hearts after ISO injection (n=6). **C.** mRNA levels of fibrosis markers in the mice hearts after ISO injection (n=6). **D.** Echocardiograph measurements in mice hearts after ISO injection (n=10). NOX4; NADPH oxidase 4, Prx-3; Peroxiredoxin-3, AAV9; adeno-associated virus 9, PSR; Picrosirius red, LV; left ventricular, ISO; Isoproterenol, and **; P<0.01 vs. control group.

NADPH oxidase 4 overexpression mitigates the anti-fibrosis effects of peroxiredoxin-3

First, we injected the mice with AAV9-NOX4 and AAV9-Prx-3 to overexpress cardiac NOX4 and Prx-3, followed by an ISO injection (Fig.5A). The LV collagen volume was increased in the AAV9-NOX4+ AAV9-Prx-3 group compared with the AAV9-Prx-3 group (Fig.5B). Transcription of those fibrosis markers increased in the AAV9-NOX4+ AAV9-Prx-3 group compared with the AAV9-Prx-3 group (Fig.5C). Echocardiography evaluation of cardiac function showed decreased levels of LVEF, LVFS and E/A in the ISO group compared with the NS group (Fig.5D). Overall, these findings indicate that NOX4 overexpression can counter the anti-fibrosis effects of Prx-3.

Discussion

Cardiac fibrosis embodies a stress response after a heart injury, and can lead to myocardial remodelling and heart pump failure (17). CFs are key cells in the occurrence and development of myocardial fibrosis, and the main source cells of the extracellular matrix. CFs can activate and

differentiate into myofibroblasts, which secrete a-SMA contractile protein during myocardial injury induced by various cardiovascular diseases (18). Excessive activation of myofibroblasts leads to adverse cardiac remodelling and heart failure (19). In this study, we provide previously undocumented evidence that Prx-3 can inhibit ISO-induced cardiac fibrosis and protect against cardiac dysfunction. Our findings indicate that Prx-3 can directly affect CFs and hamper the activation, proliferation, and collagen synthesis of CFs during myocardial injury and TGFβ1 stimulation.

Prx-3 is a new member of the peroxidase family. Prx-3 is mainly located in mitochondria, which is of great significance in eliminating excessive oxidants (20). Overwhelming evidence substantiates that Prx-3 is associated with leukaemia, chemoresistance, and tumorigenesis (21). Although studies have shown that Prx-3 is important in cardiovascular diseases (10, 11), whether it plays a role in myocardial fibrosis remains largely unclear. Our study corroborated that Prx-3 directly affected TGFβ1 induced CF activation, proliferation, and collagen synthesis. Prx-3 silencing caused a deterioration in TGFβ1-induced cardiac fibroblast activation, proliferation, and collagen synthesis.

We also assessed the fibrosis pathways that may be associated with Prx-3. P38 is a member of a family of mitogen-activated protein kinases that mediate responses to extracellular stimuli and cellular function (18). P38 plays a major role in the activation of fibroblasts under external stimuli (22). Knockdown of P38α in fibroblasts prevents fibroblast activation and secretory function, thereby inhibiting fibrosis (20). During ISO-induced myocardial fibrosis, cardiomyocyte injury leads to the massive secretion of inflammatory and profibrotic factors, such as TGFβ1, and to massive activation of fibroblasts (23). There is an increasing consensus that in ISO-induced myocardial injury, the P38 gene knockout can inhibit development of myocardial fibrosis (21, 23). Thus, P38 signalling is one of the most typical regulators of fibroblast activation and myocardial fibrosis. In the present study, we found a significant increase in cardiac P38 activation in the ISO group, and Prx-3 overexpression reduced P38 activation. In addition, we found that ISO induced a significant increase in cardiac NOX4 expression, whereas Prx-3 reduced NOX4 expression. P38 is a sensory signal of oxidative stress. These data suggest that Prx-3 may inhibit P38 activation by reducing NOX4 expression and reducing cardiac oxidative stress. We observed an inhibition in Prx-3 fibrosis after transfection with an NOX4-overexpressing virus. Taken together, these findings indicate that the protective effect of Prx-3 against cardiac fibrosis is mainly mediated by NOX4-P38.

Conclusion

Overall, we found that Prx-3 could inhibit ISO-induced

cardiac dysfunction and cardiac fibrosis. Prx-3 silencing reduced TGFβ1-induced cardiac fibroblast activation, proliferation, and collagen synthesis. Prx-3 reduced NOX4 expression, thus hampering P38 activation during fibroblast activation. Therefore, Prx-3 represents a potential new target for the treatment of cardiac fibrosis.

Acknowledgements

Authors' Contributions

X.X., F.A.; Contributed to the conception and design of the experiments.J.L., Z.C., C.L., W.W.; Carried out the experiments, perform the statistic analyse and wrote the first draft of the manuscript. B.L., Y.K.; Sample preparation, analysed the experimental results and revised the manuscript. X.N., J.Z.; Re-analysed all the experimental results and statistical data, edited and revised the manuscript. All authors read and approved the final manuscript.

References

1. Tani H, Sadahiro T, Yamada Y, Isomi M, Yamakawa H, Fujita R, et al. Direct reprogramming improves cardiac function and reverses fibrosis in chronic myocardial infarction. Circulation. 2023; 147(3): 223-238.

2. Li C, Meng X, Wang L, Dai X. Mechanism of action of non-coding RNAs and traditional Chinese medicine in myocardial fibrosis: Focus on the TGF-β/Smad signaling pathway. Front Pharmacol. 2023; 14: 1092148.

3. Park S, Nguyen NB, Pezhouman A, Ardehali R. Cardiac fibrosis: potential therapeutic targets. Transl Res. 2019; 209: 121-137.

4. Li L, Zhao Q, Kong W. Extracellular matrix remodeling and cardiac fibrosis. Matrix Biol. 2018; 68-69: 490-506.

5. Motiejunaite J, Amar L, Vidal-Petiot E. Adrenergic receptors and cardiovascular effects of catecholamines. Ann Endocrinol (Paris). 2021; 82(3-4): 193-197.

6. Lavine K, Amrute J, Luo X, Penna V, Bredemeyer A, Yamawaki T, et al. Targeting immune-fibroblast crosstalk in myocardial infarction and cardiac fibrosis. Res Sq. 2023: rs.3.rs-2402606.

7. De Armas MI, Esteves R, Viera N, Reyes AM, Mastrogiovanni M, Alegria TGP, et al. Rapid peroxynitrite reduction by human peroxiredoxin 3: Implications for the fate of oxidants in mitochondria. Free Radic Biol Med. 2019; 130: 369-378.

8. Choi MH, Oh S, Choi JY, Kim JH, Lee SW. A statistical learning framework for predicting left ventricular ejection fraction based on glutathione peroxidase-3 level in ischemic heart disease. Comput Biol Med. 2022; 149: 105929.

9. Hwang I, Uddin MJ, Lee G, Jiang S, Pak ES, Ha H. Peroxiredoxin 3 deficiency accelerates chronic kidney injury in mice through interactions between macrophages and tubular epithelial cells. Free Radic Biol Med. 2019; 131: 162-172.

10. Sonn SK, Song EJ, Seo S, Kim YY, Um JH, Yeo FJ, et al. Peroxiredoxin 3 deficiency induces cardiac hypertrophy and dysfunction by impaired mitochondrial quality control. Redox Biol. 2022; 51: 102275.

11. Arkat S, Umbarkar P, Singh S, Sitasawad SL. Mitochondrial peroxiredoxin-3 protects against hyperglycemia induced myocardial damage in diabetic cardiomyopathy. Free Radic Biol Med. 2016; 97: 489-500.

12. Zong J, Li FF, Liang K, Dai R, Zhang H, Yan L, et al. Nuclear localization leucine-rich-repeat protein 1 deficiency protects against cardiac hypertrophy by pressure overload. Cell Physiol Biochem. 2018; 48(1): 75-86.

13. Jiang XH, Wu QQ, Xiao Y, Yuan Y, Yang Z, Bian ZY, et al. Evodiamine prevents isoproterenol-induced cardiac fibrosis by regulating endothelial-to-mesenchymal transition. Planta Med. 2017;

83(9): 761-769.

14. Lafuse WP, Wozniak DJ, Rajaram MVS. Role of cardiac macrophages on cardiac inflammation, fibrosis and tissue repair. Cells. 2020; 10(1): 51.

15. Li L, Yu AQ. The functional role of peroxiredoxin 3 in reactive oxygen species, apoptosis, and chemoresistance of cancer cells. J Cancer Res Clin Oncol. 2015; 141(12): 2071-2077.

16. Wu QQ, Xiao Y, Jiang XH, Yuan Y, Yang Z, Chang W, et al. Evodiamine attenuates TGF-β1-induced fibroblast activation and endothelial to mesenchymal transition. Mol Cell Biochem. 2017; 430(1-2): 81-90.

17. O'Meara E, Zannad F. Fibrosis biomarkers predict cardiac reverse remodeling. JACC Heart Fail. 2023; 11(1): 73-75.

18. Umbarkar P, Ejantkar S, Tousif S, Lal H. Mechanisms of fibroblast activation and myocardial fibrosis: lessons learned from FB-specific conditional mouse models. Cells. 2021; 10(9): 2412.

19. Osorio JM, Espinoza-Pérez C, Rimassa-Taré C, Machuca V, Bustos JO, Vallejos M, et al. Senescent cardiac fibroblasts: a key role in cardiac fibrosis. Biochim Biophys Acta Mol Basis Dis. 2023; 1869(4): 166642.

20. Molkentin JD, Bugg D, Ghearing N, Dorn LE, Kim P, Sargent MA, et al. Fibroblast-specific genetic manipulation of p38 mitogen-activated protein kinase in vivo reveals its central regulatory role in fibrosis. Circulation. 2017; 136(6): 549-561.

21. Bageghni SA, Hemmings KE, Zava N, Denton CP, Porter KE, Ainscough JFX, et al. Cardiac fibroblast-specific p38α MAP kinase promotes cardiac hypertrophy via a putative paracrine interleukin-6 signaling mechanism. FASEB J. 2018; 32(9): 4941-4954.

22. Wang L, Li S, Yao Y, Yin W, Ye T. The role of natural products in the prevention and treatment of pulmonary fibrosis: a review. Food Funct. 2021; 12(3): 990-1007.

23. Frangogiannis NG. Cardiac fibrosis. Cardiovasc Res. 2021; 117(6): 1450-1488.